

Mathematical solution for rate based model in H₂S and CO₂ absorption column using alkanolamine solutions

N.Kasiri², M.A.Ghayyem

ABSTRACT

In the present paper, a rate-based model has been developed for the simulation of H₂S and CO₂ absorption column using alkanolamine solutions. The model adopts the film theory and assumes that thermodynamic equilibrium exist only for H₂S species. The most difficulty and time consuming part in the mathematical solution of this model is determination of CO₂ and H₂S concentration in liquid film. In this research we overcame this difficulty by linear equation and matrix solution. The simulation results have been validated using available plant data. It has been found that there is a good agreement between the models computed results and plant data (Khangiran MEA and Ahvaz-1 DEA gas refinery, Iran).

KEYWORDS

H₂S and CO₂ absorption columns, Alkanolamine, MEA, DEA, Modeling, Matrix solution, concentration profiles

1. INTRODUCTION

Removal of acid gases such as CO₂ and H₂S from natural or refinery gases is an important industrial process. Monoethanolamine (MEA), diethanolamine (DEA), methyldiethanolamine (MDEA), deglycolamine (DGA) and diisopropanolamine (DIPA) are nowadays the most important alkanolamines which are used in absorption units for the removal of undesirable acid gases [1, 2].

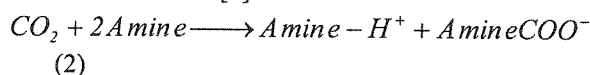
Two design approaches are in common use: the equilibrium based approach and the rate based approach. The equilibrium-based approach is suitable for nonreactive systems. For reactive systems, such as amine towers, the rate based approach is more applicable [3]. The two film theory is a rate based approach which most researchers use due to its simplicity and accuracy. Equilibrium is assumed to exist at the gas-liquid interface [2] and the film and bulk liquid solution could be assumed to be in a state of chemical equilibrium only for H₂S specie [3]. All resistances to mass transfer are assumed to be confined to two thin layers next to the interface; the gas film and the liquid film. CO₂ and H₂S in the gas bulk pass through the gas film and enter the liquid film where the reaction with amines begins. It should be noted that mass transfer and reaction with amines take place simultaneously. Reaction will continue to progress in the liquid bulk [4]. The mass fluxes at gas-liquid interface ($y=0$) and the liquid film bulk interface ($y=\delta$) is required

for calculation the amount of H₂S, CO₂ transferred to liquid and reacted by amine in each tray, which could be calculated by [5]:

$$N_i|_{z=0,\delta} = -D_i \left. \frac{dC_i}{dz} \right|_{z=0,\delta}$$

$$i = \text{CO}_2 \text{ or H}_2\text{S} \quad (1)$$

For solving, the concentration profiles of CO₂ in liquid film should be determined. The important reaction of CO₂ by amine in the film is [6]:



Therefore, concentration profile of CO₂ is obtained by:

$$D_A \frac{d^2 C_A}{dz^2} = k C_A C_B^2$$

$$A = \text{CO}_2, B = \text{amine} \quad (3)$$

Boundary conditions:

$$\text{At } z=0 \quad \frac{dC_A}{dz} = - \frac{K_g P (y_{Ab} - H'_{A} X_{Al})}{D_A} \quad \text{and}$$

$$\frac{dC_B}{dz} = 0 \quad (4)$$

$$\text{At } z=\delta \quad C_A = C_{A_b}, \quad C_B = C_{B_b}$$

Since the reaction of H₂S by amine is instantaneous and reversible, then in each cross section of liquid film and each point of liquid bulk the chemical equilibrium state exist. This equilibrium is depended on concentration of H₂S, amine and their products at each point [12].

² Computer Aided Process Engineering Lab, Chem.Eng.Dept., Iran University of Sci. & Tech., Narmak, Tehran, Iran
Email: Kasiri@iust.ac.ir, Telfax: 009821-77490416

Therefore, the concentration profile of H₂S can not be derived like CO₂ as mentioned above. Equation 3 is also difficult to solve and requires tedious calculation. Many researchers have overcome this problem by the usage of enhancement factor [2, 13], the ratio of absorption rate of solute gas in the presence of chemical reaction to that obtained with physical absorption in the liquid film. Glasscock and Rochelle [13] used a modified form of expression developed by Decoursey for the enhancement factor to model the enhancement of the mass transfer of CO₂ when it is chemically absorbed in aqueous alkanolamine solutions.

Tomcej et al.[13] used a pseudo first order model for estimating the enhancement factor for removal of CO₂ using alkanolamine, and neglected the reversibility of the chemical reaction.

Sivasubramanian [13] assumed that CO₂ enhancement factor in aqueous MDEA was equal to unity. Onda et al. [8] provide the approximate solution for the enhancement factor, who derived semi-analytical solution for the film theory by irreversible reaction.

Enhancement factors for H₂S and CO₂ in aqueous MDEA from 1 to 3 for CO₂ and 100 to 2000 for H₂S are reported [13].

Hikita and Asia [12] used the Hatta number, which divided the reaction into three regime as follows:

Hatta < 0.3 The reaction is very slow
 0.3 < Hatta < 3 The reaction is moderately fast

Hatta > 3 The reaction is very fast

Some simplification derived an analytically approximate solution for the interfacial flux and liquid film bulk flux. Onda et al. [12] derived an approximate equation for a very fast reversible reaction. Leye et al [12] assumed CO₂ reaction with alkanolamine is irreversible and of finite rate, also H₂S reaction takes place in a front inside the liquid film or at its boundaries. Consequently, all H₂S concentration profiles are linear in the film.

Taylor et al. [14,15] used finite mass transfer rates across vapor-liquid interface for modeling reactive distillation column. Kucka et al. [12] suggested a model for absorption of CO₂ by amines in packed columns. In this model, the profiles of components in liquid film were obtained by film discretization analysis.

In this paper, new model is presented for the simultaneous absorption of H₂S and CO₂ into aqueous amines, the concentration profile could be calculated precisely by new mathematical method. Effect of H₂S and CO₂ reaction products on mass transfer and chemical equilibrium in liquid film at each point has been taken into account. All equations of liquid film have been solved simultaneously.

Since no simplifying assumptions have been made, conditions regarded in the presented model are more similar to the real. Solution procedure is based on matrix method, therefore, initial guess is not required.

Consequently, the solution converged simply and very fast.

2. MATHEMATICAL MODELING

In the model the gas is assumed to be in plug flow, while the liquid on the plates is completely mixed [3]. Using the following relations molar flux and composition of the gas entering the trays are evaluated:

$$N_i|_{y=0} = K_{g,i} P_k [y_i - H'_i x_{i,k}] \quad (5)$$

$$G \frac{dy_i}{dz} = -[N_i|_{y=0} - y_i (N_A|_{y=0} + N_H|_{y=0})] A'_v \Omega_s \quad (6)$$

$$\frac{dG}{dz} = -[N_A|_{y=0} + N_H|_{y=0}] A'_v \Omega_s \quad (7)$$

$$\text{where, } H'_i = H_i C_k / P_k$$

Assuming the composition of transferred components in the liquid bulk and using the following equations, amount of liquid leaving each tray and amine composition as well as HS⁻ concentration is evaluated:

$$L_k = L_{k-1} + G_{k+1} - G_k \quad (8)$$

$$x_{B,k} L_k = x_{B,k-1} L_{k-1} - \{ \{ G_{k+1} y_{H,k+1} - G_k y_{H,k} \} - (L_k x_{H,k} - L_{k-1} x_{H,k-1}) \} + 2 \{ \{ G_{k+1} y_{A,k+1} - G_k y_{A,k} \} - (L_k x_{A,k} - L_{k-1} x_{A,k-1}) \} \quad (9)$$

$$x_{B^*,k} L_k = x_{B^*,k-1} L_{k-1} + \{ \{ G_{k+1} (y_{H,k+1} + y_{A,k+1}) - G_k (y_{H,k} + y_{A,k}) \} - [L_k (x_{H,k} + x_{A,k}) - L_{k-1} (x_{H,k-1} + x_{A,k-1})] \} \quad (10)$$

$$x_{D,k} L_k = x_{D,k-1} L_{k-1} - \{ \{ G_{k+1} y_{H,k+1} - G_k y_{H,k} \} - (L_k x_{H,k} - L_{k-1} x_{H,k-1}) \} \quad (11)$$

$$x_{B^*,k} L_k = x_{B^*,k-1} L_{k-1} + \{ \{ G_{k+1} y_{A,k+1} - G_k y_{A,k} \} - (L_k x_{A,k} - L_{k-1} x_{A,k-1}) \} \quad (12)$$

With the aid of Equations (3) and chemical equilibrium of H₂S-amine absorption at each point in the liquid film, H₂S and CO₂ concentration profiles in liquid film and composition at interface could be evaluated. H₂S-amine reaction and equilibrium equation are as follows:



$$K_{eq} = \frac{[HS^-][Amine - H^+]}{[H_2S][Amine]}$$

Finally using Equation (1) and the following equations CO₂ and H₂S composition in the liquid bulk is evaluated.

$$x_{A,k} L_k = x_{A,k-1} L_{k-1} + N_A|_{y=\delta} A'_v \Omega_s h_f - r_A (1 - A_v \delta) \Omega_s h_f \varepsilon_i \quad (14)$$

$$x_{H,k} = \frac{x_{D,k} x_{B^*,k}}{K_{eq} x_B} \quad (15)$$

Calculated quantities of composition obtained by these equations are compared with initial assumed values and iterative procedure is repeated until convergence criteria is satisfied.

The temperature distribution along the column can be calculated by:

$$T_{k,L}^{in} L_k^{in} \sum (x_{i,k}^{in} C_{P_i,i}) - T_k G_k \sum (y_{j,k} C_{P_j,j}) + T_{k,G} G_k^{in} \sum (y_{j,k}^{in} C_{P_j,i}) - T_k L_k \sum (x_{i,k} C_{P_i,i}) + \sum Q_{i,k}^{abs} - \sum Q_{i,k}^{Reac} = 0$$

3. NEW METHOD FOR EVALUATION OF CONCENTRATION PROFILE

In this method, liquid film is divided to n equal segments. In a segment, the composition of each component is considered to be the same and varies from one segment to another. In the mass continuity calculation, each interface is assumed to have the same composition as the segment to the right of it. Mass continuity equations for all components in segment 1 can be written as follows (Figure 1):

For Amine:

$$C_k D_H \left(\frac{x_{B,b} - x_{B,1}}{\Delta z} \right) - C_k D_B \left(\frac{x_{B,1} - x_{B,2}}{\Delta z} \right) = C_k D_H \left(\frac{x_{H,2} - x_{H,1}}{\Delta z} \right) - C_k D_H \left(\frac{x_{H,1} - x_{H,b}}{\Delta z} \right) + 2C_k^2 k_A x_{A,1} x_{B,1}^2 \Delta z \quad (16)$$

After rearrangement,

$$x_{B,2} - 2x_{B,1} = -x_{B,b} + 2C_k^2 k_A \frac{\Delta z^2}{D_B} x_{B,1}^2 x_{A,1} + \frac{D_H}{D_B} x_{H,2} - 2 \frac{D_H}{D_B} x_{H,1} + \frac{D_H}{D_B} x_{H,b} \quad (17)$$

For HS^- , Amine COO^- , Amine- H^+ , CO_2 , H_2S similar equations can be obtained, respectively:

$$x_{D,2} - 2x_{D,1} = -x_{D,b} - \frac{D_H}{D_D} x_{H,2} + 2 \frac{D_H}{D_D} x_{H,1} - \frac{D_H}{D_D} x_{H,b} \quad (18)$$

$$x_{B^-,2} - 2x_{B^-,1} = -x_{B^-,b} - C_k^2 k_A x_{A,1} x_{B,1}^2 \frac{\Delta z^2}{D_{B^-}} \quad (19)$$

$$x_{B^+,2} - 2x_{B^+,1} = -x_{B^+,b} - \frac{D_H}{D_{B^+}} x_{H,2} + 2 \frac{D_H}{D_{B^+}} x_{H,1} - \frac{D_H}{D_{B^+}} x_{H,b} - C_k^2 k_A \frac{\Delta z^2}{D_{B^+}} x_{B,1}^2 x_{A,1} \quad (20)$$

$$x_{A,2} - \left[2 + C_k^2 k_A \frac{\Delta z^2}{D_A} x_{B,1}^2 \right] x_{A,1} = -x_{A,b} \quad (21)$$

$$x_{H,1} = \frac{x_{D,1} x_{B^+,1}}{K_{eq} x_{B,1}} \quad (22)$$

Mass continuity equations in all segments other than 1 and n for amine, HS^- , Amine COO^- , Amine- H^+ , CO_2 , H_2S respectively are as follows:

$$x_{B,m+1} - 2x_{B,m} + x_{B,m-1} = 2C_k^2 k_A \frac{\Delta z^2}{D_B} x_{B,m}^2 x_{A,m} + \frac{D_H}{D_B} x_{H,m+1} - 2 \frac{D_H}{D_B} x_{H,m} + \frac{D_H}{D_B} x_{H,m-1} \quad (23)$$

$$x_{D,m+1} - 2x_{D,m} + x_{D,m-1} = -\frac{D_H}{D_D} x_{H,m+1} + 2 \frac{D_H}{D_D} x_{H,m} - \frac{D_H}{D_D} x_{H,m-1} \quad (24)$$

$$x_{B^-,m+1} - 2x_{B^-,m} + x_{B^-,m-1} = -C_k^2 k_A \frac{\Delta z^2}{D_{B^-}} x_{B,m}^2 x_{A,m} \quad (25)$$

$$x_{B^+,m+1} - 2x_{B^+,m} + x_{B^+,m-1} = -\frac{D_H}{D_{B^+}} x_{H,m+1} + 2 \frac{D_H}{D_{B^+}} x_{H,m} - \frac{D_H}{D_{B^+}} x_{H,m-1} - C_k^2 k_A \frac{\Delta z^2}{D_{B^+}} x_{B,m}^2 x_{A,m} \quad (26)$$

$$x_{A,m+1} - \left[2 + C_k^2 k_A \frac{\Delta z^2}{D_A} x_{B,m}^2 \right] x_{A,m} + x_{A,m-1} = 0 \quad (27)$$

$$x_{H,m} = \frac{x_{B^+,m} x_{D,m}}{K_{eq} x_{B,m}} \quad (28)$$

Mass continuity equations in segment n are as follows:

For Amine:

$$\frac{D_B}{C_k} \left(\frac{x_{B,n-1} - x_{B,n}}{\Delta z} \right) = k_g (y_{H,b} - H'_{H'} x_{H,n}) - \frac{D_H}{C_k} \left(\frac{x_{H,n} - x_{H,n-1}}{\Delta z} \right) + 2 \frac{K}{C_k^3} x_{A,n} x_{B,n}^2 \Delta z \quad (29)$$

After rearrangement,

$$x_{B,n} - x_{B,n-1} = -2k_A C_k^3 x_{A,n} x_{B,n}^2 \frac{\Delta z^2}{D_B} - \left(\frac{D_H}{D_B} + \frac{K_{g,H} H'_{H'} P_k \Delta z}{D_B C_k} \right) x_{H,n} - \frac{D_H}{D_B} x_{H,n-1} + \frac{K_{g,H} P_k \Delta z}{D_B C_k} y_{H,b} \quad (30)$$

For HS^- , Amine COO^- , Amine- H^+ , CO_2 , H_2S similar equations can be obtained respectively:

$$x_{D,n} - x_{D,n-1} + \left(\frac{D_H}{D_D} + \frac{K_{g,H} H'_{H'} P_k \Delta z}{D_D C_k} \right) x_{H,n} - \frac{D_H}{D_D} x_{H,n-1} = \frac{K_{g,H} P_k \Delta z}{C_k D_D} y_{H,b} \quad (31)$$

$$x_{B^-,n} - x_{B^-,n-1} = C_k^2 k_A x_{A,n} x_{B,n}^2 \frac{\Delta z^2}{D_{B^-}} \quad (32)$$

$$x_{B^+,n} - x_{B^+,n-1} = C_k^2 k_A \frac{\Delta z^2}{D_{B^+}} x_{A,n} x_{B,n}^2 - \left(\frac{D_H}{D_{B^+}} + \frac{K_{g,H} H'_{H'} P_k \Delta z}{D_{B^+} C_k} \right) x_{H,n} + \frac{D_H}{D_{B^+}} x_{H,n-1} + K_{g,H} P_k \frac{\Delta z}{D_{B^+} C_k} y_{H,b} \quad (33)$$

$$\left[K_{g,A} H'_{H'} P_k \frac{\Delta z}{D_A C_k} + 1 + C_k^2 k_A x_{B,n}^2 \frac{\Delta z^2}{D_A} \right] x_{A,n} - x_{A,n-1} = K_{g,A} P_k \frac{\Delta z}{D_A C_k} y_{A,b} \quad (34)$$

$$x_{H,n} = \frac{x_{B^+,n} x_{D,n}}{K_{eq} x_{B,n}} \quad (35)$$

4. SOLUTION PROCEDURE

The applied solution method is a simple and accurate one. Initially H_2S and amine concentrations have been assumed in each segment. This provides a set of diagonally dominant equations, the solution of which give x_{HS^-} , $x_{Amine-H^+}$, $x_{AmineCOO^-}$, x_{CO_2} , x_{Amine} and x_{H_2S} values. Since amine concentration in solution is very high compared with other components and H_2S reaches to equilibrium state in every position instantaneously, it is easier to assume these components initial values. In the meanwhile, using these assumptions decrease calculation time and give more accurate results.

Mole fractions in all segments have been calculated using Equations 16-35. For calculation of HS⁻ concentration profile, equations 18, 24, 31 are rearranged and the following matrix is derived:

$$\begin{bmatrix} -2 & 1 & 0 & 0 & \dots & \dots & \dots & \dots & \dots & \dots & 0 \\ 1 & -2 & 1 & 0 & \dots & \dots & \dots & \dots & \dots & \dots & 0 \\ 0 & 1 & -2 & 1 & 0 & \dots & \dots & \dots & \dots & \dots & 0 \\ \vdots & \vdots & \vdots & \vdots & \vdots & \vdots & \vdots & \vdots & \vdots & \vdots & \vdots \\ 0 & \dots & \dots & \dots & 0 & 1 & -2 & 1 & 0 & \dots & 0 \\ \vdots & \vdots & \vdots & \vdots & \vdots & \vdots & \vdots & \vdots & \vdots & \vdots & \vdots \\ 0 & \dots & \dots & \dots & \dots & \dots & \dots & 0 & 1 & -2 & 1 \\ 0 & \dots & \dots & \dots & \dots & \dots & \dots & 0 & 0 & -1 & 1 \end{bmatrix} \begin{bmatrix} x_{D,1} \\ x_{D,2} \\ \vdots \\ x_{D,m} \\ \vdots \\ x_{D,n} \end{bmatrix} = \begin{bmatrix} -x_{D,b} - \frac{D_H}{D_D} x_{H,2} + 2 \frac{D_H}{D_D} x_{H,1} - \frac{D_H}{D_D} x_{H,b} \\ -\frac{D_H}{D_D} x_{H,3} + 2 \frac{D_H}{D_D} x_{H,2} - \frac{D_H}{D_D} x_{H,1} \\ \vdots \\ -\frac{D_H}{D_D} x_{H,m+1} + 2 \frac{D_H}{D_D} x_{H,m} - \frac{D_H}{D_D} x_{H,m-1} \\ \vdots \\ -\left(\frac{D_H}{D_D} + \frac{F'}{D_D}\right) x_{H,m} + \frac{D_H}{D_D} x_{H,m-1} + \frac{G}{D_D} y_{H,b} \end{bmatrix} \quad (36)$$

where, $F' = K_{g,H} H'_H P_k \frac{\Delta Z}{C_k}$ and $G = K_{g,H} P_k \frac{\Delta Z}{C_k}$.

For other components similar matrix equations are developed (for more details refer to Appendix A).

5. PHYSICOCHEMICAL PROPERTIES AND MODEL PARAMETERS:

In gas phase calculations, the compressibility factor of non ideal gas (Z) is evaluated from dranchuck et al method [16]. Gas diffusivity coefficients and gas viscosity are calculated from modified Hirschfelder-Bird-Spotz and Underling methods, respectively [17, 18].

Mounik method is applied for the evaluation of the interfacial area per unit froth volume on the sieve plate as follows [19]:

$$A_v' = (233.15 + 55.69u_g - 536.6h_i) \left(\frac{\rho_l}{1140}\right)^{0.45} \left(\frac{2.36}{\mu_l}\right)^{0.12} \left(\frac{0.078}{\sigma}\right)^{0.33} \quad (37)$$

The physical mass transfer coefficient in the liquid and gas is determined by Grester et al, as follows [19]:

$$K_g a = 2.0350 * 10^4 D_A^{0.5} (1 - \varepsilon) [0.40u_g (\rho_g)^{0.5} + 0.15] \quad (38)$$

$$K_g a = \frac{G_M}{Ph_f Sc_g^{0.5}} (0.776 + 4.567h_w - 0.238u_g (\rho_g)^{0.5} + \frac{104.9V_l}{Z_l}) \quad (39)$$

Liquid viscosity and density are determined by Pohorecki et al and Meisen et al methods, respectively [19]. Henry and specific heat coefficients are evaluated by

Kent et al and Prausnitz et al methods, respectively [20,16]. Diffusivity of CO₂ in liquid phase is calculated from Barret and danckwerts method as follows [19]:

$$(D_w \mu_w)_T = (D_A \mu_A)_T \quad (40)$$

$$\log D_w = -8.1764 + \frac{712.5}{T} - \frac{2.591 \times 10^5}{T^2} \quad (41)$$

H₂S diffusivity in liquid phase is calculated from Wilke & Chang method [17]. Film thickness is evaluated by modified correlation, using heat and mass transfer analogy as follows [21]:

$$\delta = \frac{0.024h_f}{(n_1^{0.8} + n_2^a)} \left(\frac{Z_l h_w \mu_l}{V_l \rho_l}\right)^{0.50} \left(\frac{\rho_l D_{l,CO_2}}{\mu_l}\right)^{0.33} \quad (42)$$

where, a is 1.3 for very fast reaction, 1 for moderately fast reaction and 0.8 for very slow reaction. In the above equation, the number of the components which enter the liquid film or leave it and take place in the reaction is " n_2 " but without reaction is " n_1 ".

6. RESULTS AND DISCUSSION

Using the developed model a simulation program has been prepared for H₂S and CO₂ absorption column by alkanolamine. Concentration profiles of reaction products and feed components along the column, calculated by this program are compared with a MEA and DEA plant data. Feed and Amine specifications of Khangiran, MEA, and Ahvaz-1, DEA, gas refinery plants are presented in Table 1.

Concentration profile for H₂S, CO₂ in gas and liquid phase, also amine concentration profile in liquid phase and temperature distribution in column (for these two plant), experimental data and simulated result are presented in Figure 4-13.

For these plants data set, a good agreement between simulated result and experimental data for the gas and liquid phase concentrations and temperature profile, can be observed. It should be noted that no adaptive parameters are used for the simulation with the model. Simulation of MEA data set is of special interest, since this model was able to describe the process properly as shown in Figures 4-8. In MEA absorption plant, the concentration of H₂S at outlet gas for experimental and simulated values are 2×10^{-6} and 3.25×10^{-6} respectively. These values for CO₂ are 9×10^{-6} and 12×10^{-6} respectively. This good agreement between experimental and simulated values is based on new mathematical method leads to good estimation of concentration profiles in liquid film. This model needs less initial assumption, has linear equation, has simple and fast calculation because of using matrix method (no complexity) converges rapidly and excellently.

Calculation of this concentration profiles, using numerical method, is more complex. Because equation (3)

and its boundary condition (4) is a boundary value problem. In order to solve this equation by numerical method we need to convert it to initial value problem, therefore it required some initial guess and more iteration. Convergence depends on initial guess, proper tolerance and numerical method for integration of second order differential equation.

Concentration variation of components in the liquid film at the top of the column (tray 3) and at the bottom of it (tray 18) is depicted in Figures 2 and 3. At the top of the column, since CO₂ and H₂S concentration in gas phase is low, mass transfer decreases and amine, OH⁻ and H⁺ concentration do not change along the liquid film (Figure 2) contrary to what is seen for the bottom of the column in Figure 3. According to these figures, amine concentration could be assumed to be almost constant along the liquid film. This is obviously due to the high concentration of amine entire the column.

H₂S concentration profile in gas phase along the column for the simulated and real MEA plant is represented in Figure 4. According to this figure, H₂S mole fraction decreases sharply at stages 20-14 then drops down mildly to almost zero as we approach the top of the tower. It hinges upon the fact that, concentration of H₂S and consequently driving force for mass transfer at the bottom of the column is more than the top of it and the reaction is instantaneously. The same result has been obtained for CO₂ (Figure 3). Figure 1 has been revealed that MEA has tendency to absorb CO₂ similar to H₂S; however it is not enough for selective absorption of CO₂. Mole fractions of H₂S and CO₂ in the gas stream leaving the column are 6×10^{-6} and 9×10^{-9} respectively which means that standard values of H₂S and CO₂ concentrations are achieved and other complementary processes need not to be applied.

Mole fractions of H₂S and CO₂ in the liquid phase for MEA plant are shown in Figures 6 and 7. Analysis of these figures is the same as what mentioned for Figures 4 and 5. Temperature variation along the column for MEA plant is depicted in Figure 8. Since all occurring reactions are exothermic and most of H₂S and CO₂ are absorbed at column bottom trays, temperature variation is very high in these trays. Initial variation in temperature curve trend at tray 20 is due to lower temperature of input gas rather than column bottom temperature. According to Figures 4-8, it has been found that simulation and plant data are compatible with each other, excellently.

The corresponding plots for Ahvaz-1 DEA field data are shown in Figures 9-13. It is clear from these figures that the model predictions are in concordance with plant data, except for trays 13-19 in some of these figures. This incompatibility is due to the reaction between water and CO₂ and consequently production of HCO₃⁻ which has not taken into account in simulator. It should be noted that absorption of CO₂ with water is negligible compared with that of with DEA and specially MEA.

7. CONCLUSION

In this work, a mathematical model and a solution algorithm based on the rate approach is presented, which can be used to design and simulate an acid gas absorption tower using aqueous solution of alkanolamine. In the present model, a new method of mathematics is applied for evaluation of CO₂ and H₂S concentration profiles to overcome shortcomings of complexity, non convergence and to improve accuracy of simulated result. Using this model, components concentration profiles of more exactness with simple calculations have been obtained; convergence of solution algorithm became faster than the exist numerical method; solution algorithm became precise and simple and finally problem of solving nonlinear equations with nonhomogenous conditions has been resolved. A good agreement between the plant data and simulated values for the gas and liquid composition and temperature distribution along the column, demonstrated a sufficient predictivity of the proposed model for the gas sweetening process.

Table 1- Feed and Amine specifications of Khangiran and Ahvaz-1 gas refinery plants

	Khangiran		Ahvaz-1	
	Feed	Amine	Feed	Amine
Pressure (psi)	627	615	418	410
Temperature (°C)	40	60	40	60
Flow rate (kmol/hr)	7500	47000	5096	59750
H ₂ S mole fraction	0.0211	0.0003	0.0196	0.0003
CO ₂ mole fraction	0.0455	0.0014	0.0630	0.0014
MEA mole fraction	-	0.0660	-	-
DEA mole fraction	-	-	-	0.0658
Feed introduction tray	20		20	



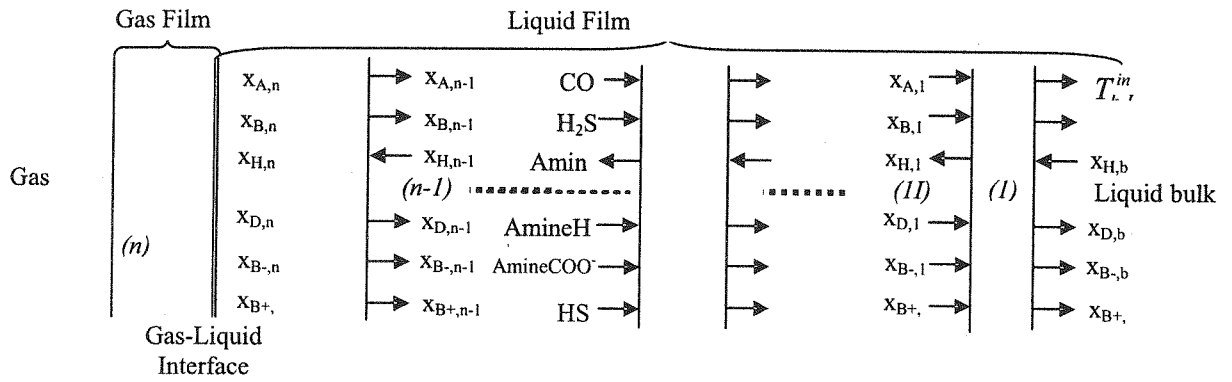


Figure 1- Transferred components in liquid and gas film and its boundary condition

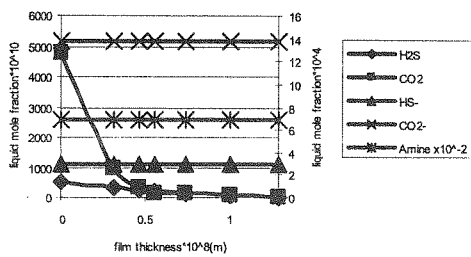


Figure 2- Concentration variation of components at tray 3

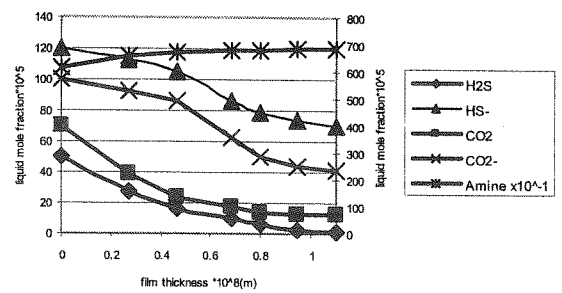


Figure 3- Concentration variation of components at tray 18

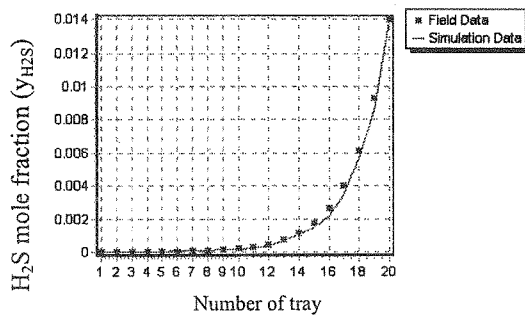


Figure 4- H₂S mole fraction variation in gas phase along the column (MEA plant)

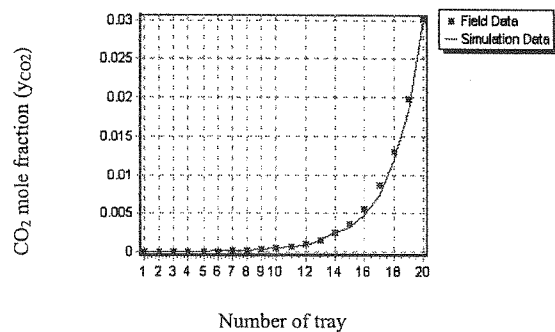


Figure 5- CO₂ mole fraction variation in gas phase along the column (MEA plant)

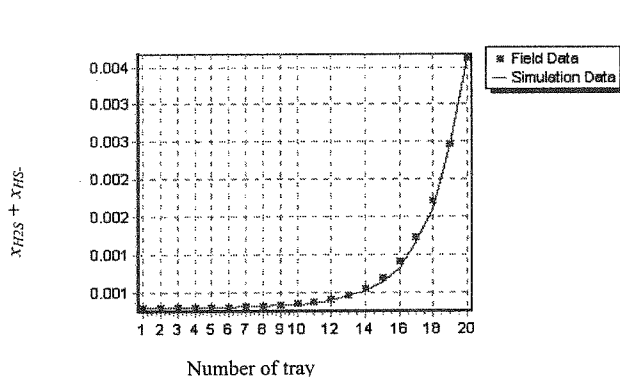


Figure 6- Mole fraction of H₂S + HS⁻ in liquid phase along the column (MEA plant)

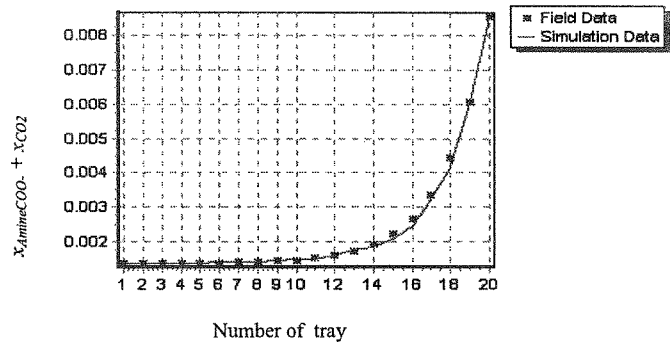


Figure 7- Mole fraction of AmineCOO⁻ + CO₂ in liquid phase along the column (MEA plant)



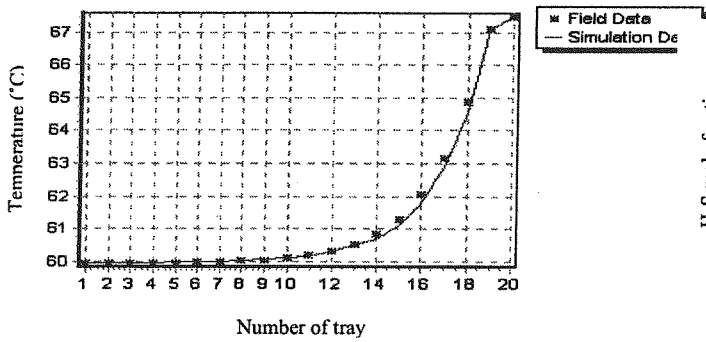


Figure 8- Temperature distribution along the column (MEA plant)

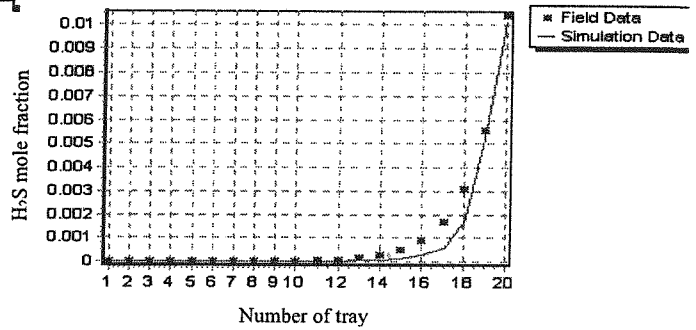


Figure 9- H₂S mole fraction variation in gas phase along the column (DEA plant)

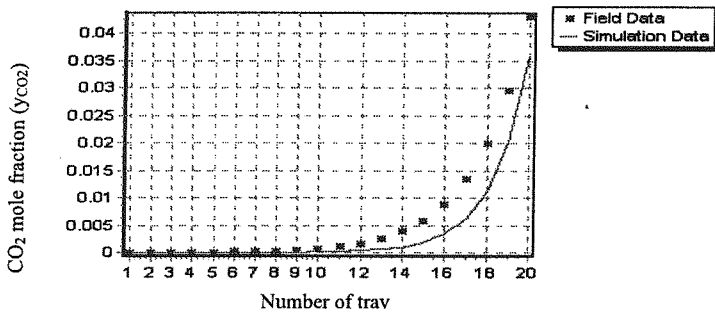


Figure 10- CO₂ mole fraction variation in gas phase along the column (DEA plant)

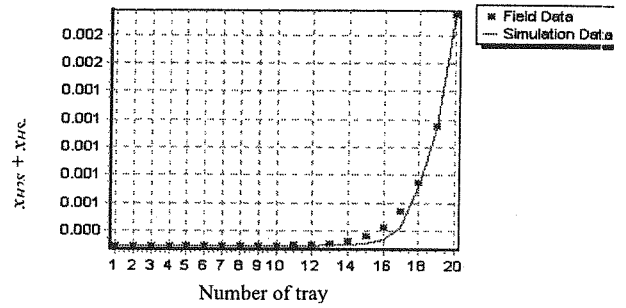


Figure 11- Mole fraction of H₂S + HS⁻ in liquid phase along the column (DEA plant)

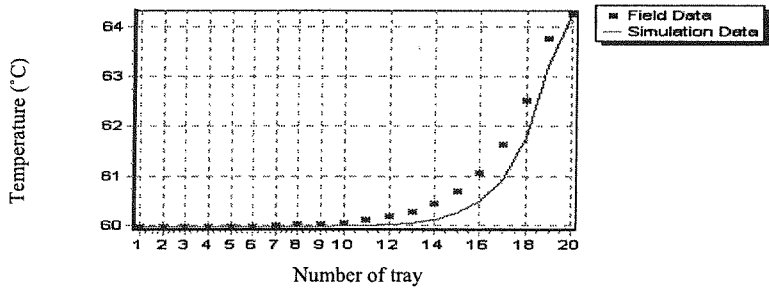


Figure 12- Mole action of AmineCOO⁻ + CO₂ in liquid phase along the column (DEA plant)

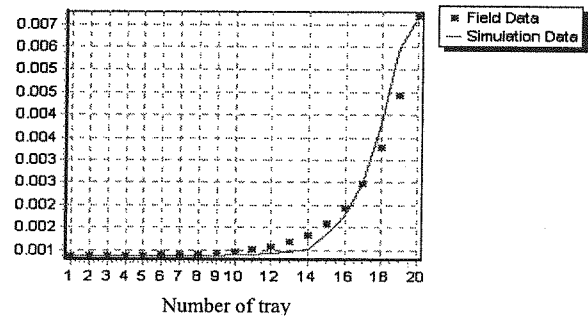


Figure 13- Temperature distribution along the column (DEA plant)

8. APPENDIX A

For AmineCOO⁻: M2*S3=R3

For Amine-H⁺: M2*S4=R4

For Amine: M2*S5=R5

For H₂S: S6=R6



$$M2 = \begin{bmatrix} -2 & 1 & 0 & 0 & \dots & \dots & \dots & \dots & \dots & \dots & 0 \\ 1 & -2 & 1 & 0 & \dots & \dots & \dots & \dots & \dots & \dots & 0 \\ 0 & 1 & -2 & 1 & 0 & \dots & \dots & \dots & \dots & \dots & 0 \\ \vdots & \vdots & \vdots & \vdots & \vdots & \vdots & \vdots & \vdots & \vdots & \vdots & \vdots \\ 0 & \dots & \dots & \dots & 0 & 1 & -2 & 1 & 0 & \dots & 0 \\ \vdots & \vdots & \vdots & \vdots & \vdots & \vdots & \vdots & \vdots & \vdots & \vdots & \vdots \\ 0 & \dots & \dots & \dots & \dots & \dots & 0 & 1 & -2 & 1 \\ 0 & \dots & \dots & \dots & \dots & \dots & 0 & 0 & -1 & 1 \end{bmatrix}$$

$$S3 = \begin{bmatrix} x_{B^-,1} \\ x_{B^-,2} \\ \vdots \\ x_{B^-,m} \\ \vdots \\ x_{B^-,n} \end{bmatrix}$$

$$S4 = \begin{bmatrix} x_{B^+,1} \\ x_{B^+,2} \\ \vdots \\ x_{B^+,m} \\ \vdots \\ x_{B^+,n} \end{bmatrix}$$

$$S5 = \begin{bmatrix} x_{B,1} \\ x_{B,2} \\ \vdots \\ x_{B,m} \\ \vdots \\ x_{B,n} \end{bmatrix}$$

$$S6 = \begin{bmatrix} x_{H,1} \\ x_{H,2} \\ x_{H,3} \\ \vdots \\ x_{H,m} \\ \vdots \\ x_{H,n} \end{bmatrix}$$

$$R3 = \begin{bmatrix} -x_{B^-,b} - \frac{A'}{D_{B^-}} x_{B,1}^2 x_{A,1} \\ -\frac{A'}{D_{B^-}} x_{B,2}^2 x_{A,2} \\ \vdots \\ -\frac{A'}{D_{B^-}} x_{B,m}^2 x_{A,m} \\ \vdots \\ \frac{A'}{D_{B^-}} x_{B,n}^2 x_{A,n} \end{bmatrix}$$

$$R4 = \begin{bmatrix} -x_{B^+,b} - \frac{D_H}{D_{B^+}} (x_{H,2} - 2x_{H,1} + x_{H,b}) - \frac{A'}{D_{B^+}} x_{B,1}^2 x_{A,1} \\ -\frac{D_H}{D_{B^+}} (x_{H,3} - 2x_{H,2} + x_{H,1}) - \frac{A'}{D_{B^+}} x_{B,2}^2 x_{A,2} \\ \vdots \\ -\frac{D_H}{D_{B^+}} (x_{H,m+1} - 2x_{H,m} + x_{H,m-1}) - \frac{A'}{D_{B^+}} x_{B,m}^2 x_{A,m} \\ \vdots \\ \frac{A'}{D_{B^+}} x_{B,n}^2 x_{A,n} - \left(\frac{D_H}{D_{B^+}} + \frac{F'}{D_{B^+}} \right) x_{H,n} + \frac{D_H}{D_{B^+}} x_{H,n-1} + \frac{G}{D_{B^+}} y_{H,b} \end{bmatrix}$$

$$R5 = \begin{bmatrix} -x_{B,b} + 2\frac{A'}{D_B} x_{B,1}^2 x_{A,1} + \frac{D_H}{D_B} (x_{H,2} - 2x_{H,1} + x_{H,b}) \\ 2\frac{A'}{D_B} x_{B,2}^2 x_{A,2} + \frac{D_H}{D_B} (x_{H,3} - 2x_{H,2} + x_{H,1}) \\ \vdots \\ 2\frac{A'}{D_B} x_{B,m}^2 x_{A,m} + \frac{D_H}{D_B} (x_{H,m+1} - 2x_{H,m} + x_{H,m-1}) \\ \vdots \\ -2\frac{A'}{D_B} x_{B,n}^2 x_{A,n} + \left(\frac{D_H}{D_B} + \frac{F'}{D_B} \right) x_{H,n} - \frac{D_H}{D_B} x_{H,n-1} - \frac{G}{D_B} y_{H,b} \end{bmatrix}$$

$$R6 = \begin{bmatrix} x_{D,1} x_{B^-,1} / K_{eq} x_B \\ x_{D,2} x_{B^-,2} / K_{eq} x_B \\ x_{D,3} x_{B^-,3} / K_{eq} x_B \\ \vdots \\ x_{D,m} x_{B^-,m} / K_{eq} x_B \\ \vdots \\ x_{D,n} x_{B^-,n} / K_{eq} x_B \end{bmatrix}$$

Where, $A' = k_A C_k^2 \Delta z^2$.

For CO₂:

$$\begin{bmatrix} -(2 + \frac{A'}{D_A} x_{B,1}^2) & 1 & 0 & 0 & \dots & \dots & \dots & 0 \\ 1 & -(2 + \frac{A'}{D_A} x_{B,2}^2) & 1 & 0 & \dots & \dots & \dots & 0 \\ 0 & 1 & (-2 + \frac{A'}{D_A} x_{B,3}^2) & 1 & \dots & \dots & \dots & 0 \\ 0 & 0 & \dots & \dots & \dots & \dots & \dots & \vdots \\ \vdots & \vdots & \vdots & \vdots & \vdots & \vdots & \vdots & \vdots \\ 0 & \vdots & \vdots & \vdots & \vdots & \vdots & \vdots & \vdots \\ \vdots & \vdots & \vdots & \vdots & \vdots & \vdots & \vdots & \vdots \\ 0 & \dots & \dots & \dots & \dots & \dots & -1 & (\frac{B'}{D_A} + 1 + \frac{A'}{D_A} x_{B,n}^2) \end{bmatrix} \begin{bmatrix} x_{A,1} \\ x_{A,2} \\ x_{A,3} \\ \vdots \\ x_{A,m} \\ \vdots \\ x_{A,n} \end{bmatrix} = \begin{bmatrix} -x_{A,b} \\ 0 \\ \vdots \\ 0 \\ \vdots \\ 0 \\ \vdots \\ Ey_{A,b} \end{bmatrix} \quad (M4)$$

Where, $B' = K_{g,A} H_A' P_k \frac{\Delta z}{C_k}$ and $E = K_{g,A} \frac{P_k}{C_k} \frac{\Delta z}{D_A}$.

9. NOMENCLATURE

A'_v	Gas-liquid interfacial area per unit volume froth on the plate (m^{-1})
A_v	Gas-liquid interfacial area per unit liquid volume on the plate (m)
B	Amine
B'	AmineCOO ⁻
B^+	AmineH ⁺
C	Molar concentration ($kmol\ m^{-3}$)
D	Molecular diffusivity ($m^2\ h^{-1}$)
G	Molar gas flow rate ($kmol\ h^{-1}$)
G_m	Molar gas flow rate per unit plate area ($kmol\ m^{-2}\ s^{-1}$)
H	Henry's coefficient ($bar\ m^3\ kmol^{-1}$)
h_f	Froth height on the plate (m)
h_w	Weir height (m)
h_l	Clear liquid height (m)
K_{eq}	Equilibrium constant
K_l	Liquid mass transfer coefficient for absorbed component (m/h)
K_g	Gas mass transfer coefficient for absorbed component ($kmol\ m^{-2}\ h^{-1}\ bar^{-1}$)
k	Reaction rate coefficient ($m^3\ kmol^{-1}\ h^{-1}$)
L	Molar liquid flow rate ($kmol\ h^{-1}$)
N	Molar flux ($kmol\ m^{-2}\ h^{-1}$)
P	Pressure (bar)
r_A	Reaction rate of component A ($kmol\ m^{-3}\ h^{-1}$)
Sc	Schmidt Number
T	Temperature (K)
$T_{k,L}^m$	Temperature of liquid inlet to k tray (K)
$T_{k,G}^m$	Temperature of liquid inlet to k tray (K)
u	Linear velocity (mh^{-1})
V	Volume flow rate ($m^3\ h^{-1}$)
x	Mole fraction in the liquid stream
y	Mole fraction in the gas stream
z	Axial coordinate (m)
Z_i	Average width of liquid flow on the plate (m)
ΔZ	Segment thickness in liquid film (m)
ϵ_l	Liquid fraction in the froth
σ	Surface tension ($N\ m^{-1}$)
δ	Liquid film thickness (m)
Ω	Cross section area of tower (m^2)
Ω_a	Active area of plate (m^2)
ρ	Density (kg/m^3)
μ	Viscosity ($mpa.s$)
Subscripts	
A	CO ₂
b	Bulk
D	HS ⁻
g	Gas
H	H ₂ S
I	Gas-liquid interface
i	Component
k	Plate number
l	Liquid
w	Water

10. REFERENCES

- [1] W. Hu, A. Chakma, "Modeling of equilibrium solubility of CO₂ and H₂S in aqueous diglycolamine (DGA) solutions", The Canadian Journal of Chemical Engineering, Vol. 68, June, (1990).
- [2] N. A. Al-Baghli, S. A. Pruess, V. F. Yesavage, M. S. Selim, "A rate-based model for the design of gas absorbers for the removal of CO₂ and H₂S using aqueous solution of MEA and DEA", Fluid Phase Equilibria 185 31-43, (2001).
- [3] L. De Leye and G. F. Froment, "Rigorous simulation and design of columns for gas absorption and chemical reaction-II", Computer & Chemical Engineering, Vol. 10, No. 5, pp. 505-515, (1986).
- [4] E. Y. Keing, R. Schneider, A. Gorak, "Multicomponent unsteady-state film model: A general analytical solution to the linearized diffusion-reaction problem", Chemical Engineering Journal 83, 85-94, (2001).
- [5] E. Rascol, M. Meyer, M. Pervost, "Simulation and parameter sensitivity analysis of acid gas absorption into mixed alkanolamine solutions", Computers Chem. Engng Vol. 20, Suppl., pp. S1401-S1406, (1996).
- [6] C. P. Escollbillana, J. A Saez, J. R. Perez- Correa and H. J. Neuburg, Behavior of absorption/stripping columns for the CO₂-MEA system; Modeling and experiments, The Canadian Journal of Chemical Engineering, Vol. 69, August, pp.969-977, (1991).
- [7] A. E. Cornelissen, "Simulation of absorption of H₂S and CO₂ into aqueous alkanolamines in tray and packed columns", Koninklijke/Shell-Laboratorium, Institution of Chemical Engineers, Amsterdam, vol. 58, pp242-250, (1980).
- [8] R. D. Vas Bhat, W. P. M. Van Swaaji, J. A. M. Kuipers, G. F. Versteeg, "Mass transfer with complex chemical reaction in gas-liquid systems-I: Consecutive reversible reactions with equal diffusivities", Chemical Engineering Science 54, 121-136, (1999).
- [9] R. D. Vas Bhat, W. P. M. Van Swaaji, J. A. M. Kuipers, G. F. Versteeg, "Mass transfer with complex chemical reaction in gas-liquid systems-II: Effect of unequal diffusivities on consecutive reactions", Chemical Engineering Science 54, 137-147, (1999).
- [10] A. A. Shaikh, U. A. Al-Mubaiyedh, "On the bulk-liquid reaction in isothermal reactive gas absorption", Chemical Engineering Journal 70, 65-70, (1998).
- [11] H. Bosch, G. H. Versteeg, W. P. M. Van Swaaji, "Gas liquid mass transfer with parallel reversible reactions-I: Absorption of CO₂ into solutions of sterically hindered amines", Chemical Engineering Science, Vol. 44, No. 11, pp. 2723-2734, (1989).
- [12] L. Kucka, I. Muller, E. Y. Kenig, A. Gorak, "On the modeling and simulation of sour gas absorption by aqueous amine solutions, Chemical Engineering Science 58, 3571-3578, (2003).
- [13] M. A. Pacheco, G. T. Rochelle, rate based modeling of reactive absorption of CO₂ and H₂S into aqueous methyl di ethanol amine, Ind. Eng. Chem. Res. Vol.37, No.10, pp4107-4117, (1998).
- [14] R. Taylor, R. Krishna, review modeling reactive distillation, Chem. Eng. Sci. 55, pp5183-5229,(2000).
- [15] R. Baur, A. P. Higler, R. Taylor, R. Krishna, comparison of equilibrium stage and non equilibrium stage models for reactive distillation. Chem. Eng. J., 76, pp33-47, (2000).
- [16] B. E. Poling, J. M. Prasnitz, J. M. O'Connell, "The properties of gases and liquids", 5th Ed. McGraw-Hill publication, (2000).
- [17] R. E. Treybal, "Mass transfer operation", 3rd Ed. McGraw-Hill publication, (1980).
- [18] W. D. Mc Cain, "The properties of petroleum fluid", 2nd Ed. Pennwell Books, (1990).
- [19] R. Phorecki, W. Moniuk, "Plate efficiency in the process of absorption with chemical reaction-experiments and example calculations", Elsevier Sequoia, printed in the Netherlands, (1988).
- [20] R. L. Kent, B. Eisenberg, "Better data for amine treating", Hydrocarbon Processing, pp87-90, (1976).
- [21] M. Becker, "Heat transfer a modern approach", Plenum Press, New York, 1st Ed (1986).